Proton radii for muonic hydrogen spectroscopy from lattice QCD

Miguel Salg, Dalibor Djukanovic, Georg von Hippel, Harvey B. Meyer, Konstantin Ottnad, Hartmut Wittig

LATTICE 2024, August 2, 2024

JOHANNES GUTENBERG UNIVERSITÄT MAINZ

PRISMA+

MPA MAINZ PHYSICS ACADEMY

Outline

Motivation

- "Proton radius puzzle": discrepancy between different determinations of the electric and magnetic radii of the proton
- In lattice QCD as in the context of scattering experiments: electromagnetic radii extracted from slope of corresponding form factors at $Q^2 = 0$
- Tension between Q^2-dependence of form factors from different experiments

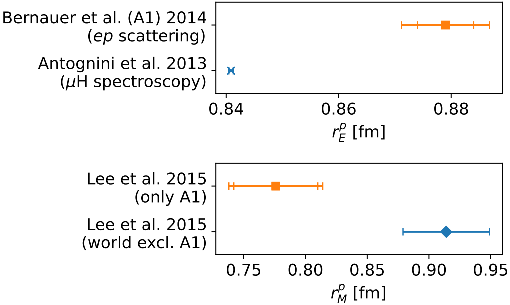

- Accurate determination of proton radii from muonic hydrogen spectroscopy ⇒ other definitions of radii, not previously computed on the lattice, become relevant
- Upcoming high-precision measurements of hyperfine splitting in muonic hydrogen by FAMU and CREMA

Motivation

- Lamb shift
  - LO proton-structure contribution: electric radius
  - NLO: two-photon exchange, dominated by elastic part, depends on third Zemach moment[1],

$$\langle r_E^3 \rangle_{(2)}^p = \frac{24}{\pi} \int_0^\infty \frac{dQ^2}{(Q^2)^{5/2}} \left[(G_E^p(Q^2))^2 - 1 + \frac{1}{3} \langle r_E^2 \rangle^p Q^2 \right] \tag{1}$$

  - Associated radius: Friar radius, $r_F^p = \sqrt[3]{\langle r_E^3 \rangle_{(2)}^p}$
- Hyperfine splitting (HFS)
  - LO proton-structure contribution: Zemach radius[2],

$$r_Z^p = -\frac{2}{\pi} \int_0^\infty \frac{dQ^2}{(Q^2)^{3/2}} \left(\frac{G_E^p(Q^2) G_M^p(Q^2)}{\mu_M^p} - 1 \right) \tag{2}$$

  - First-principles prediction of Zemach radius could be checked by high-precision experiments

[1] Friar 1979 [Ann. Phys. **122**, 151]; [2] Zemach 1956 [Phys. Rev. **104**, 1771].

Outline

Ensembles

Coordinated Lattice Simulations (CLS)[3]

- Non-perturbatively $\mathcal{O}(a)$-improved Wilson fermions, $N_f = 2+1$
- $\mathrm{tr}\, M_q = 2m_l + m_s =$ const.
- Tree-level improved Lüscher-Weisz gauge action
- $\mathcal{O}(a)$-improved conserved vector current

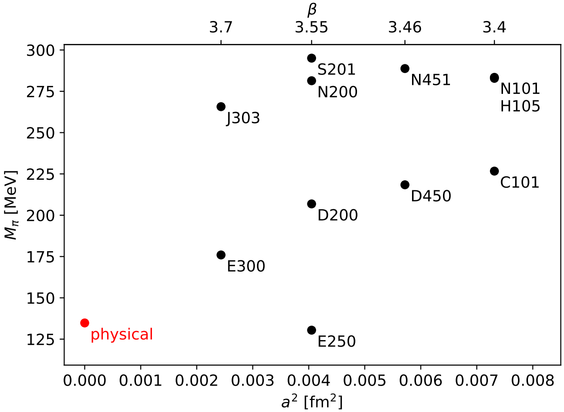

Figure: Overview of the ensembles used in this study

[3]Bruno et al. 2015 [JHEP **2015** (2), 43]; Bruno, Korzec, and Schaefer 2017 [PRD **95**, 074504].

Nucleon two- and three-point correlation functions

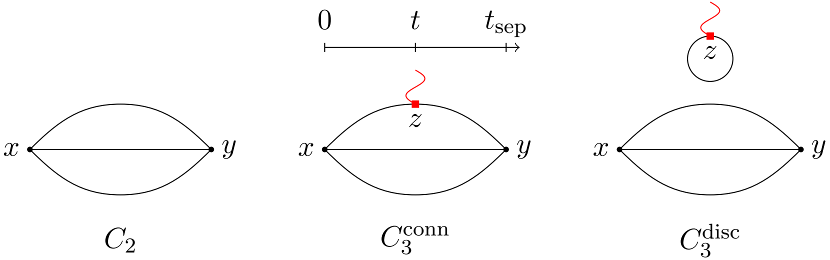

- Measure the two- and three-point correlation functions of the nucleon
- For three-point functions, Wick contractions yield connected and disconnected contribution
- Compute the quark loops via a stochastic estimation using a frequency-splitting technique[4]
- Extract the effective form factors $G_{E,M}^{\mathrm{eff}}$ using the ratio method[5]

[4] Giusti et al. 2019 [EPJC **79**, 586]; Cè et al. 2022 [JHEP **2022** (8), 220]; [5] Korzec et al. 2009 [PoS **066**, 139].

Excited-state analysis

- Summation method: parametric suppression of excited-state effects ($\propto e^{-\Delta t_\mathrm{sep}}$ instead of $\propto e^{-\Delta t}$, $e^{-\Delta(t_\mathrm{sep}-t)}$ [Δ: energy gap to lowest-lying excited state])
- Apply LO summation method with varying starting values $t_\mathrm{sep}^\mathrm{min}$ for the linear fit (ground-state form factor = slope as function of t_sep)
- Perform a weighted average over $t_\mathrm{sep}^\mathrm{min}$, where the weights are given by a smooth window function[6],

$$\hat{G} = \frac{\sum_i w_i G_i}{\sum_i w_i}, \qquad w_i = \tanh\frac{t_i - t_w^\mathrm{low}}{\Delta t_w} - \tanh\frac{t_i - t_w^\mathrm{up}}{\Delta t_w}, \tag{3}$$

  where t_i is the value of $t_\mathrm{sep}^\mathrm{min}$ in the i-th fit, $t_w^\mathrm{low} = 0.9\,\mathrm{fm}$, $t_w^\mathrm{up} = 1.1\,\mathrm{fm}$ and $\Delta t_w = 0.08\,\mathrm{fm}$
- Reliable detection of the plateau with reduced human bias (same window on all ensembles)
- Conservative error estimate

[6] Djukanovic et al. 2022 [PRD **106**, 074503]; Agadjanov et al. 2023 [PRL **131**, 261902].

Excited-state analysis

- Summation method: parametric suppression of excited-state effects ($\propto e^{-\Delta t_{\mathrm{sep}}}$ instead of $\propto e^{-\Delta t}$, $e^{-\Delta(t_{\mathrm{sep}}-t)}$ [Δ: energy gap to lowest-lying excited state])
- Apply LO summation method with varying starting values $t_{\mathrm{sep}}^{\mathrm{min}}$ for the linear fit

D450 ($M_\pi = 218$ MeV, $a = 0.076$ fm)

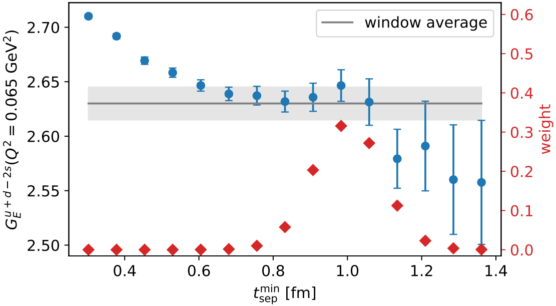

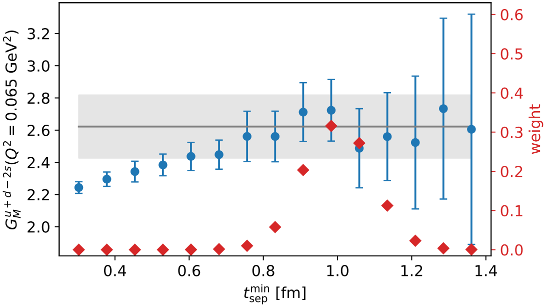

[6] Djukanovic et al. 2022 [PRD **106**, 074503]; Agadjanov et al. 2023 [PRL **131**, 261902].

Excited-state analysis

- Summation method: parametric suppression of excited-state effects ($\propto e^{-\Delta t_{\text{sep}}}$ instead of $\propto e^{-\Delta t}$, $e^{-\Delta(t_{\text{sep}}-t)}$ [Δ: energy gap to lowest-lying excited state])
- Apply LO summation method with varying starting values $t_{\text{sep}}^{\text{min}}$ for the linear fit (ground-state form factor = slope as function of t_{sep})
- Perform a weighted average over $t_{\text{sep}}^{\text{min}}$, where the weights are given by a smooth window function[6],

$$\hat{G} = \frac{\sum_i w_i G_i}{\sum_i w_i}, \qquad w_i = \tanh \frac{t_i - t_w^{\text{low}}}{\Delta t_w} - \tanh \frac{t_i - t_w^{\text{up}}}{\Delta t_w}, \tag{3}$$

where t_i is the value of $t_{\text{sep}}^{\text{min}}$ in the i-th fit, $t_w^{\text{low}} = 0.9\,\text{fm}$, $t_w^{\text{up}} = 1.1\,\text{fm}$ and $\Delta t_w = 0.08\,\text{fm}$

- Reliable detection of the plateau with reduced human bias (same window on all ensembles)
- Conservative error estimate

[6] Djukanovic et al. 2022 [PRD **106**, 074503]; Agadjanov et al. 2023 [PRL **131**, 261902].

Direct Baryon χPT fits

- Combine parametrization of the Q^2-dependence with the chiral, continuum, and infinite-volume extrapolation
- Use expressions from covariant baryon chiral perturbation theory[7] to perform simultaneous fit to the pion-mass, Q^2-, lattice-spacing, and finite-volume dependence of the form factors
- Include contributions from the ρ (ω and ϕ) mesons in the isovector (isoscalar) channel
- Reconstruct proton and neutron observables from separate fits to the isovector and isoscalar form factors
- Perform fits with various cuts in M_π and Q^2, as well as with different models for the lattice-spacing and finite-volume dependence, in order to estimate systematic uncertainties
- Large number of degrees of freedom $\Rightarrow$ improved stability against lowering the Q^2-cut
- Compute Zemach and Friar radii directly at physical point rather than on each ensemble

[7] Bauer, Bernauer, and Scherer 2012 [PRC **86**, 065206].

Outline

Extrapolation of the form factors

- BχPT including vector mesons only trustworthy for $Q^2 \lesssim 0.6\,\text{GeV}^2$
- Tail of the integrands suppressed (estimate see below)
- Extrapolate BχPT fit results using a z-expansion[8] *ansatz*,

$$G_E^{p,n}(Q^2) = \sum_{k=0}^{9} a_k^{p,n} z(Q^2)^k, \quad G_M^{p,n}(Q^2) = \sum_{k=0}^{9} b_k^{p,n} z(Q^2)^k, \tag{4}$$

where

$$z(Q^2) = \frac{\sqrt{\tau_{\text{cut}} + Q^2} - \sqrt{\tau_{\text{cut}} - \tau_0}}{\sqrt{\tau_{\text{cut}} + Q^2} + \sqrt{\tau_{\text{cut}} - \tau_0}} \tag{5}$$

- We fix $G_E^p(0) = a_0^p = 1$ and $G_E^n(0) = a_0^n = 0$, and use $\tau_{\text{cut}} = 4M_{\pi,\text{phys}}^2$ and $\tau_0 = 0$
- Incorporate large-Q^2 constraints on form factors[9] (4 sum rules for each form factor[10])

[8] Hill and Paz 2010 [PRD **82**, 113005]; [9] Lepage and Brodsky 1980 [PRD **22**, 2157]; [10] Lee, Arrington, and Hill 2015 [PRD **92**, 013013].

Integration

- For integration, smoothly replace BχPT parametrization of the form factors by z-expansion-based extrapolation ($\Delta Q_w^2 = 0.1\,\mathrm{GeV}^2$),

$$F(Q^2) = \frac{1}{2}\left[1 - \tanh\left(\frac{Q^2 - Q_{\mathrm{cut}}^2}{\Delta Q_w^2}\right)\right] F^{\chi}(Q^2) + \frac{1}{2}\left[1 + \tanh\left(\frac{Q^2 - Q_{\mathrm{cut}}^2}{\Delta Q_w^2}\right)\right] F^{z}(Q^2), \tag{6}$$

where $F(Q^2) \equiv G_E(Q^2)G_M(Q^2)/\mu_M$ for r_Z and $F(Q^2) \equiv G_E^2(Q^2)$ for $\langle r_E^3\rangle_{(2)}$, resp.

Integration: integrands for the proton

- For integration, smoothly replace BχPT parametrization of the form factors by z-expansion-based extrapolation ($\Delta Q_w^2 = 0.1\,\text{GeV}^2$)

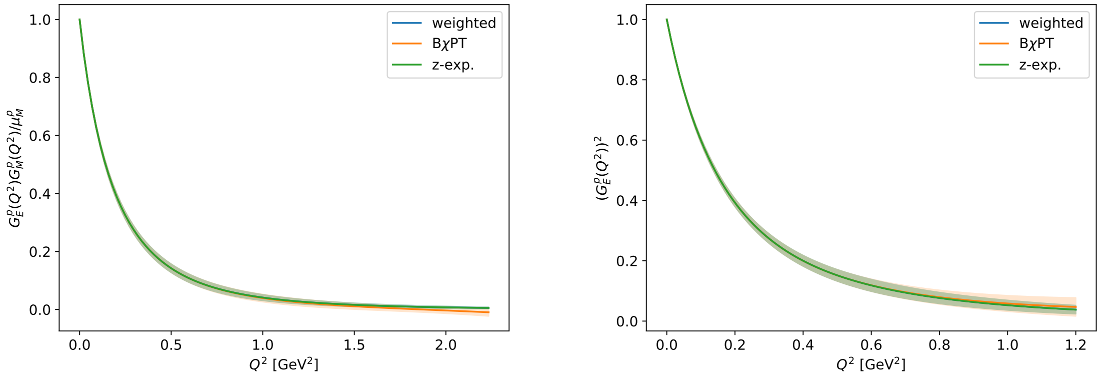

Integration

- For integration, smoothly replace BχPT parametrization of the form factors by z-expansion-based extrapolation ($\Delta Q_w^2 = 0.1\,\mathrm{GeV}^2$),

$$F(Q^2) = \frac{1}{2}\left[1 - \tanh\left(\frac{Q^2 - Q_{\mathrm{cut}}^2}{\Delta Q_w^2}\right)\right] F^{\chi}(Q^2) + \frac{1}{2}\left[1 + \tanh\left(\frac{Q^2 - Q_{\mathrm{cut}}^2}{\Delta Q_w^2}\right)\right] F^{z}(Q^2), \tag{6}$$

  where $F(Q^2) \equiv G_E(Q^2)G_M(Q^2)/\mu_M$ for r_Z and $F(Q^2) \equiv G_E^2(Q^2)$ for $\langle r_E^3\rangle_{(2)}$, resp.
- Estimate contribution of the form factors at $Q^2 > Q_{\mathrm{cut}}^2$ by setting $F^z(Q^2) \equiv 0$
- Contribution of FFs above $0.6\,\mathrm{GeV}^2$ to r_Z^p less than $0.9\,\%$, to $\langle r_E^2\rangle_{(2)}^p$ less than $0.3\,\%$
- Cancellation between different terms of the integrand for $\langle r_E^3\rangle_{(2)}^p$ at small Q^2 does not occur at the required numerical accuracy on all bootstrap samples
- Regulate integral from $Q^2 = 0$ to $Q^2 = 0.01\,\mathrm{GeV}^2$ by replacing $t_0 Q^2 \to t_0 Q^2 + \epsilon$ in the denominator, $\epsilon = 1 \cdot 10^{-7} \Rightarrow$ change in $\langle r_E^3\rangle_{(2)}^p$ by less than $0.06\,\sigma$

Outline

Model average

- Perform a weighted average over the results of all fit variations, using weights derived from the Akaike Information Criterion[11],

$$w_i = \exp\left(-\frac{1}{2}\mathrm{BAIC}_i\right) \bigg/ \sum_j \exp\left(-\frac{1}{2}\mathrm{BAIC}_j\right) , \quad \mathrm{BAIC}_i = \chi^2_{\mathrm{noaug,min},i} + 2n_{f,i} + 2n_{c,i}, \tag{7}$$

  where n_f is the number of fit parameters and n_c the number of cut data points
- Strongly prefers fits with low n_c, *i.e.*, the least stringent cut in Q^2 $\Rightarrow$ apply a flat weight over the different Q^2-cuts to ensure strong influence of our low-momentum data
- Determine the final cumulative distribution function (CDF) from the weighted sum of the bootstrap distributions[12]
- Quote median of this CDF together with the central $68\,\%$ percentiles

[11] Akaike 1974 [IEEE Trans. Autom. Contr. **19**, 716]; Neil and Sitison 2022 [arXiv:2208.14983]; [12] Borsányi et al. 2021 [Nature **593**, 51].

Results for Zemach radii and third Zemach moments

- r_Z^p: low value favored, but agrees within $2\,\sigma$ with most other determinations (except for dispersive analysis)
- $\langle r_E^3 \rangle_{(2)}^p$: low value favored, good agreement with dispersive analysis, clear tension with A1
- Our estimates are $\sim 86\,\%$ and $\sim 97\,\%$, respectively, correlated with electric proton radius
- Low results for r_Z^p and $\langle r_E^3 \rangle_{(2)}^p$ expected, no independent puzzle

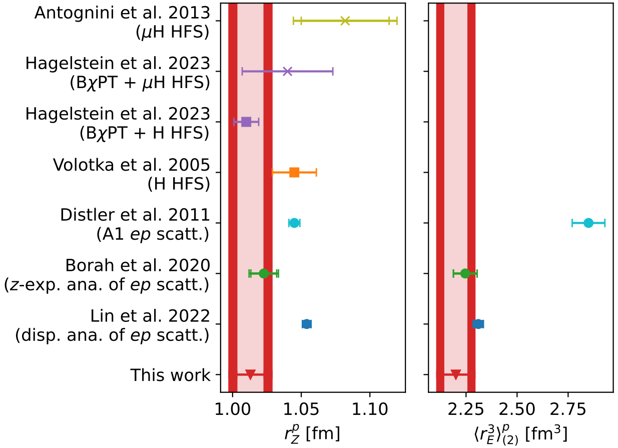

- Neutron results agree with z-expansion analysis of world en-scattering data, larger error

Correlations between different proton radii

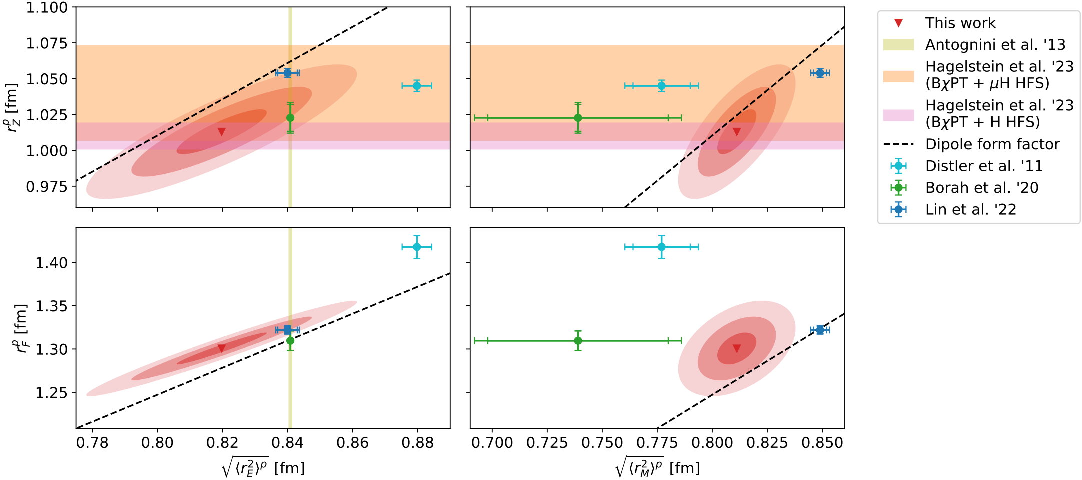

Lattice results seem to confirm trends observed in data-driven evaluations

Outline

1. Motivation
2. Lattice setup and form factor calculation [PRD **109**, 094510]
3. Zemach and Friar radii from the lattice [PRD **110**, L011503]
4. Model average and final results
5. Conclusions and outlook

Conclusions

- Determination of Zemach and Friar radii of the proton and neutron from lattice QCD
- Based on calculation of the electromagnetic form factors which includes connected and disconnected contributions, as well as a full error budget
- Precision of proton radii sufficient to allow meaningful comparison to data-driven evaluations
- Small values for Zemach and Friar radii of the proton favored
- Large correlation with electromagnetic radii
- Good agreement with dispersive approaches for electric properties of the proton (electric and Friar radii), tension regarding its magnetic properties (magnetic and Zemach radii)
- Further investigations required, in particular for the proton's magnetic and Zemach radii
- Goal: complete and consistent picture of all electromagnetic properties of the nucleon

Backup slides

From correlation functions to form factors

- Average over the forward- and backward-propagating nucleon and over x-, y-, and z-polarization for the disconnected part
- Calculate the ratios

$$R_{V_\mu}(\mathbf{q}; t_{\mathrm{sep}}, t) = \frac{C_{3,V_\mu}(\mathbf{q}; t_{\mathrm{sep}}, t)}{C_2(\mathbf{0}; t_{\mathrm{sep}})} \sqrt{\frac{\bar{C}_2(\mathfrak{q}; t_{\mathrm{sep}} - t) C_2(\mathbf{0}; t) C_2(\mathbf{0}; t_{\mathrm{sep}})}{C_2(\mathbf{0}; t_{\mathrm{sep}} - t) \bar{C}_2(\mathfrak{q}; t) \bar{C}_2(\mathfrak{q}; t_{\mathrm{sep}})}}, \tag{8}$$

where $t_{\mathrm{sep}} = y_0 - x_0$, $t = z_0 - x_0$, and $\bar{C}_2(\mathfrak{q}; t_{\mathrm{sep}}) = \sum_{\tilde{\mathbf{q}} \in \mathfrak{q}} C_2(\tilde{\mathbf{q}}; t_{\mathrm{sep}}) \Big/ \sum_{\tilde{\mathbf{q}} \in \mathfrak{q}} 1$

- At zero sink momentum, the effective form factors can be computed from the ratios as

$$G_E^{\mathrm{eff}}(Q^2; t_{\mathrm{sep}}, t) = \sqrt{\frac{2E_{\mathbf{q}}}{m + E_{\mathbf{q}}}} R_{V_0}(\mathbf{q}; t_{\mathrm{sep}}, t), \tag{9}$$

$$G_M^{\mathrm{eff}}(Q^2; t_{\mathrm{sep}}, t) = \sqrt{2E_{\mathbf{q}}(m + E_{\mathbf{q}})} \frac{\sum_{j,k} \epsilon_{ijk} q_k \operatorname{Re} R_{V_j}^{\Gamma_i}(\mathbf{q}; t_{\mathrm{sep}}, t)}{\sum_{j \neq i} q_j^2} \tag{10}$$

Excited-state analysis: window average on E300

E300 ($M_\pi = 176$ MeV, $a = 0.049$ fm)

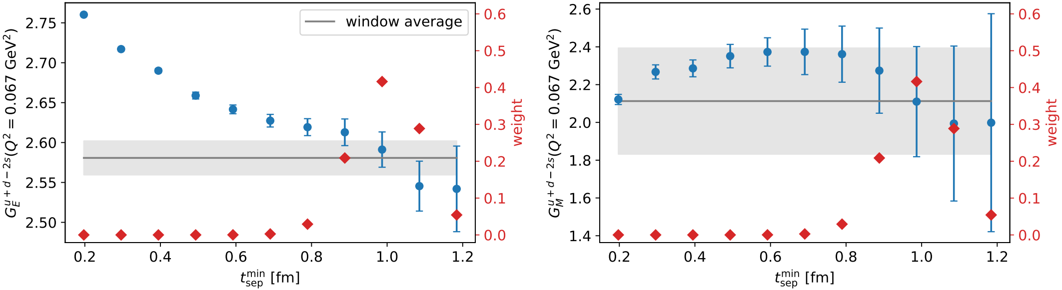

Q^2-dependence of the isovector form factors on E300

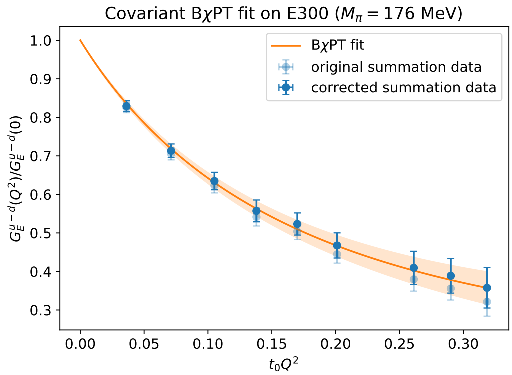

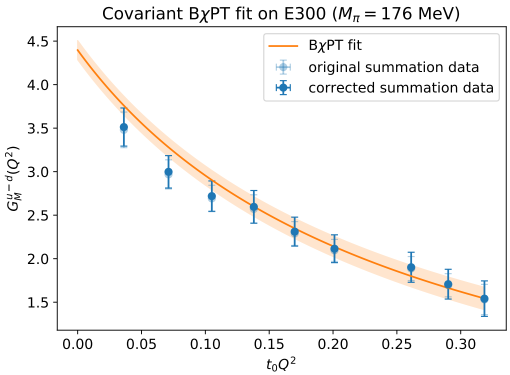

- Direct BχPT fit describes data very well
- Reduced error due to the inclusion of several ensembles in one fit

Q^2-dependence of the isoscalar form factors on E300

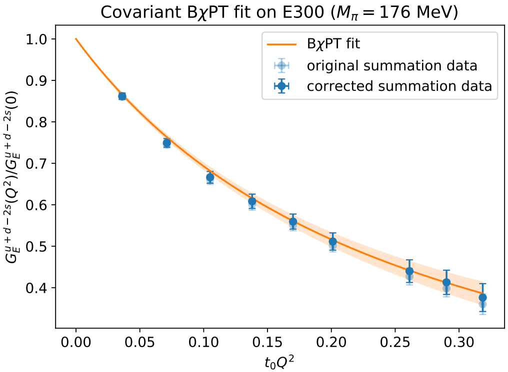

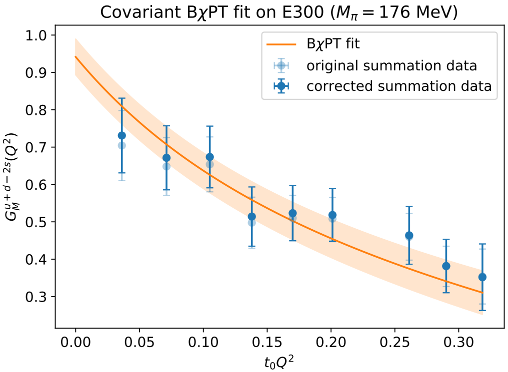

Q^2-dependence of the isovector form factors on E250

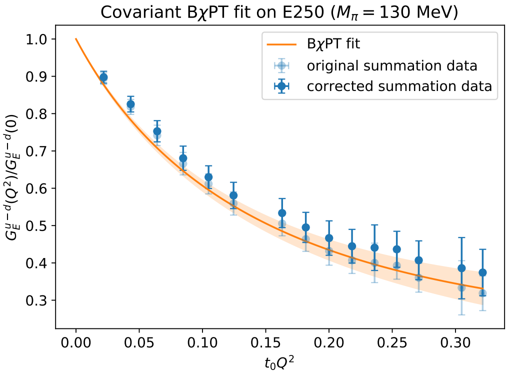

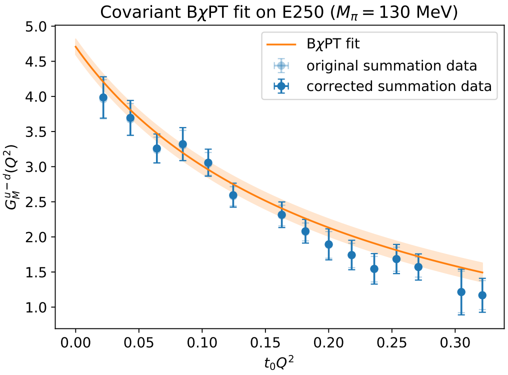

Q^2-dependence of the isoscalar form factors on E250

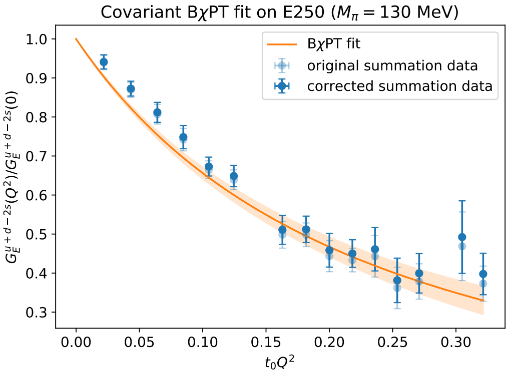

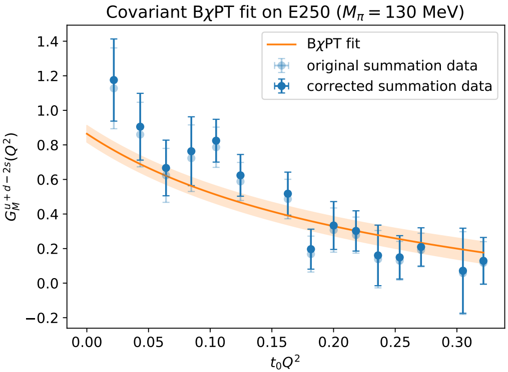

Residuals of the BχPT fits

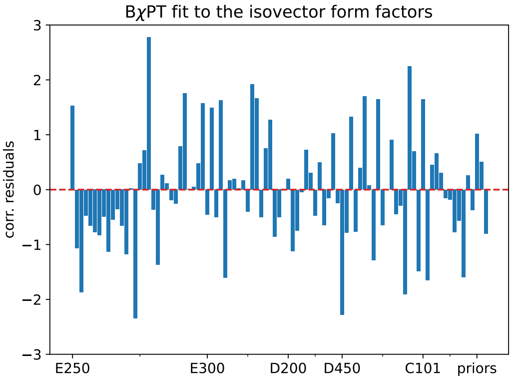

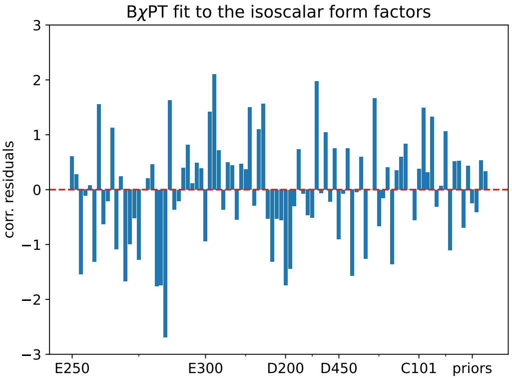

Histograms

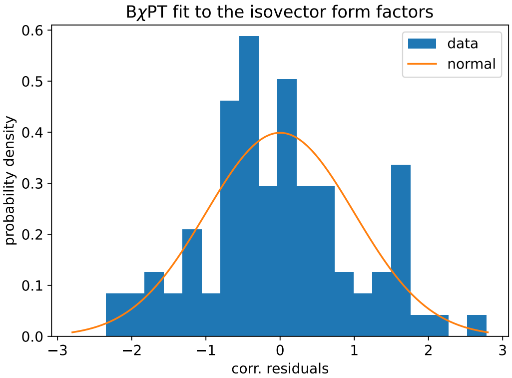
BχPT fit to the isovector form factors
data
normal
probability density
corr. residuals
0.0
0.1
0.2
0.3
0.4
0.5
0.6
−3
−2
−1
0
1
2
3

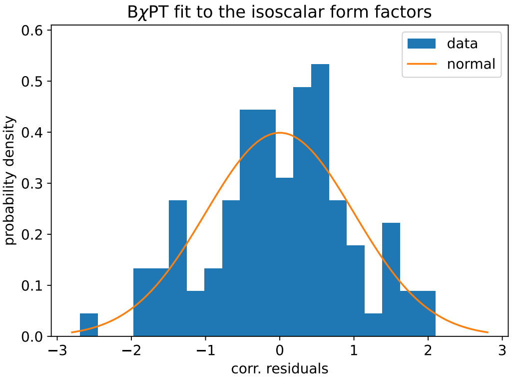
BχPT fit to the isoscalar form factors
data
normal
probability density
corr. residuals
0.0
0.1
0.2
0.3
0.4
0.5
0.6
−3
−2
−1
0
1
2
3

Q-Q plots

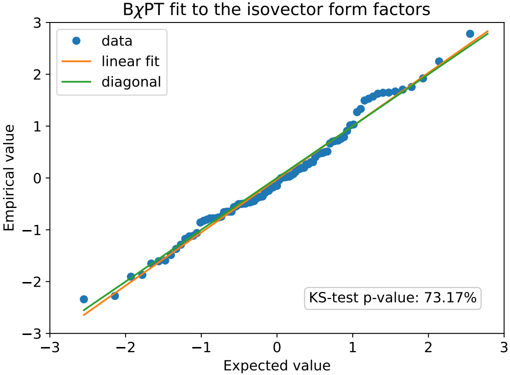

BχPT fit to the isovector form factors
data
linear fit
diagonal
KS-test p-value: 73.17%
Empirical value
Expected value

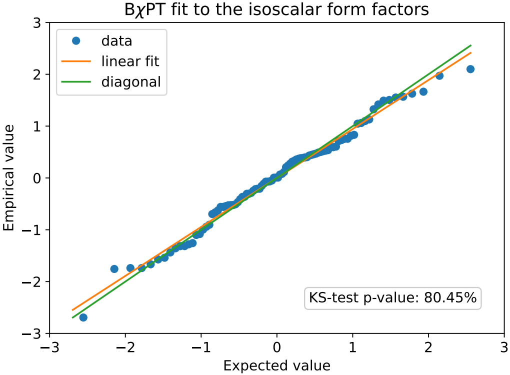

BχPT fit to the isoscalar form factors
data
linear fit
diagonal
KS-test p-value: 80.45%
Empirical value
Expected value

Integrands for the Zemach radius and third Zemach moment of the neutron

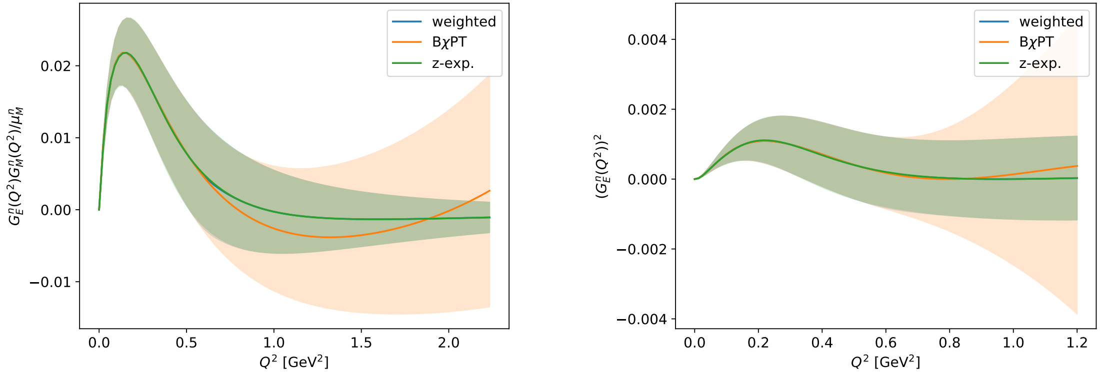

- BχPT clearly not reliable for large Q^2
- z-expansion agrees well with BχPT parametrization in region where it is fitted

Disambiguating the statistical and systematic uncertainties

- Scale the statistical variances of the individual fit results by a factor of $\lambda = 2$
- Repeat the model averaging procedure
- Assumptions:
  - Above rescaling only affects the statistical error of the averaged result
  - Statistical and systematic errors add in quadrature
- Contributions of the statistical and systematic errors to the total error,

$$\sigma_{\mathrm{stat}}^2 = \frac{\sigma_{\mathrm{scaled}}^2 - \sigma_{\mathrm{orig}}^2}{\lambda - 1}, \qquad \sigma_{\mathrm{syst}}^2 = \frac{\lambda\sigma_{\mathrm{orig}}^2 - \sigma_{\mathrm{scaled}}^2}{\lambda - 1} \tag{11}$$

- Consistency check: results are almost independent of λ (if it is chosen not too small)

Correlations between different proton radii

- Estimate covariance matrix of model-averaged results for different proton radii r_j,

$$C_{jk} = \frac{1}{(\mathrm{cdf}_{\mathcal{N}}^{-1}(3/4))^2}\,\mathrm{med}([r_j - \mathrm{med}(r_j)][r_k - \mathrm{med}(r_k)]), \quad \mathrm{corr}_{jk} = C_{jk}/\sqrt{C_{jj}C_{kk}} \tag{12}$$

- Calculate median from model-averaged (empirical) CDF
- We obtain as correlation matrix of $[\sqrt{\langle r_E^2\rangle^p}, \sqrt{\langle r_M^2\rangle^p}, r_Z^p, r_F^p]$,

$$\mathrm{corr} = \begin{pmatrix} 1 & 0.41294995 & 0.85702489 & 0.97214447 \\ 0.41294995 & 1 & 0.72010978 & 0.42834371 \\ 0.85702489 & 0.72010978 & 1 & 0.79974042 \\ 0.97214447 & 0.42834371 & 0.79974042 & 1 \end{pmatrix} \tag{13}$$

- Approximate model-averaged distribution as multivariate Gaussian with above covariance matrix in vicinity of central values $\rightarrow$ plot confidence ellipses